Low Energy Excitations and Desorption Dynamics from Oxide Surfaces

M. Menges[1], *B. Baumeister*[1], *K. Al-Shamery*[1], *B. Adam*[1], *Th. Mull*[1], *H.-J. Freund*[1], *C. Fischer*[2], *D. Weide*[2], *and P. Andresen*[2]

[1]Lehrstuhl für Physikalische Chemie I, Ruhr-Universiät Bochum, W-4630 Bochum, Germany

[2]Max-Planck-Institut für Strömungsforschung, Bunsenstr. 10, W-3400 Göttingen, Germany

1. Introduction

The interaction of photons with solid surfaces initiates processes which may be classified into various categories [1,2]. We will be concerned mainly with photochemical processes, including desorption of participating molecules. The measurement of the distribution of energy into translational and internal degrees of freedom possibly provides us with new insights into the mechanisms underlying the desorption after photoabsorption. In order to study the simplest cases first, various groups have studied photodesorption of NO and CO from metal and metaloxide surfaces [3-17]. A whole range of photon energies has been used so far. It appears that if we exclude photoinduced thermal desorption, the cross sections for photodesorption are orders of magnitude larger on weakly oxidized metal surfaces and in particular on oxide surfaces than on metal surfaces. Qualitatively, several effects are responsible for this difference in our view.

i) The electronic structure of the substrates is considerably different in the sense that a metal does not exhibit a band gap while an oxide often does. Energy that is dissipated into the substrate must exceed the gap energy in the case of an oxide unless there are defect states filling the gap. For a metal energy in any small quantity may be dissipated into the solid because excitation of electron-hole pairs of low energy is always possible. The probability of such excitations depends of course on the density of states at the Fermi energy. Metals with low density of states, such as Cu, Ag, Au, etc. should have a smaller probability for electron-hole-pair-creation.

ii) The degree of localization of the electronic charge distribution is typical for an oxide, while delocalization is a prototype metal property. This leads in the case of an oxide to a longer lifetime of the excited state. Consequently, the probability to escape the surface is larger for photodesorption from oxide surfaces due to the possibility to accumulate translational energy to leave the surface [13-15].

iii) A weak molecule-surface interaction will favour localization of the excitation on the molecule and thus increase the photodesorption probability.

Indeed the highest photodesorption cross-sections are observed for weakly bound molecules on oxide surfaces [13-17].The relatively large desorption cross sections allow us to simultaneously measure the energy distribution onto internal and translational degrees of freedom of the desorbing particles applying laser techniques. From the results of the studies we can deduce certain aspects of the mechanism of photodesorption through computer modelling of the complex experimental data.

We review in the following our experimental setup as well as the results on some of the adsorbate systems.

2. Experimental setup

Fig. 1 shows a schematic diagram of our experimental setup. A desorption laser, in our case an ArF-excimer laser with 6.4 eV photon energy, is fired normal towards the surface for about

Springer Series in Surface Sciences, Vol. 31
Desorption Induced by Electron Transitions DIET V
Editors: A.R. Burns · E.B. Stechel · D.R. Jennison

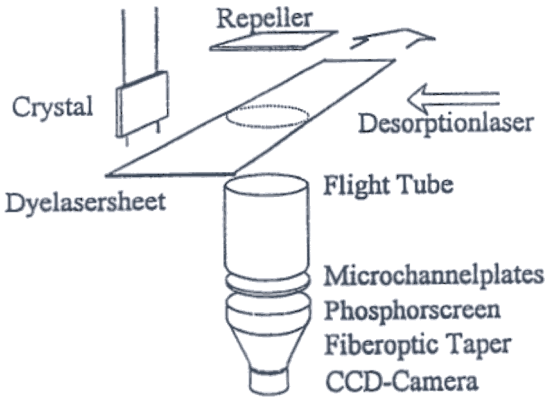

Fig.1. Schematic representation of the experimental setup.

15 nsec. The molecules that escape from the surface are detected after a given time delay of the order of μsec with a resonant multiphoton ionisation (REMPI) detection system.

The REMPI signal is induced by an excimer laser pumped dye laser system fired parallel to the surface. The illuminated area may either form a line or be spread into a sheet perpendicular to the surface with a cylindrical lens system. In each point of the illuminated area the desorbing molecules undergo an excitation and ionisation (1+1) process. Via these processes the molecules resulting from a well defined rotational-vibrational state are converted into ions. These ions are than repelled into a flight tube perpendicular to both the probe and desorption laser and are detected with a multichannel array. An image may be detected on the phosphorous screen behind the multichannel plates which is recorded by a videocamera and a personal computer. This image represents a distribution of time-of-flights because each line in the laser sheet is equivalent to a well defined distance from the surface. Simultaneously, one records the angular dependence of desorption along the lines parallel to the surface. One needs about three to four "shots" to record an image.

However, at the present time the signal-to-noise is limited in such images, which makes the identification of weak features difficult. We redose the surface after each laser shot by applying a background pressure of $5*10^{-8}$ Torr and take the difference between the REMPI signals with and without desorption which gives us the desorption signal. If we are interested in precise time-of-flight data we use the REMPI system without imaging and record the signal generated from a laser line by varying the time delay between the desorption and the probe laser [18].

Other groups have used imaging techniques to study desorption [10]. However, the laser sheet used in those studies was oriented parallel to the surface in order to determine the angular distribution of the desorbing molecules. In most other studies non-imaging detection has been employed and while we have mostly employed a desorption energy of 6.4 eV other groups have studied desorption at energies, which cover the region from 1.25 eV to 6.5 eV (see for example [1,2]).

3. Results and Discussion

3.1 The adsorbate systems NO on NiO (100) and on NiO(111)

The adsorption of NO and CO on well defined NiO surfaces has so far only been studied by very few groups [16,17,19] in contrast to NiO powder samples where numerous studies have been reported (see for example [20]).

We have used thin NiO films of (100) and (111) orientation grown on Ni(100) and Ni(111) single crystal metal surfaces [21,22]. With these samples all standard electron spectroscopic methods for adsorbate charactarization may be applied. The oxide surfaces exhibit reasonable long range order leading to LEED patterns and STM images compatible with oxide terraces of 100x150 Å width in the case of NiO(100).

On the terraces of NiO(100), NO adsorbs on top of the Ni ions with the NO axis tilted by 45° with respect to surface normal as revealed by NEXAFS. This is also supported by ab initio calculations [19]. HREELS shows that the vibrational frequency of the NO stretch is close to the gas phase value of NO which is typical for adsorption on oxide surfaces. The binding

energy is 0.5 eV (peak desorption temperature T_p = 200 K) , which is in the regime of weak chemisorption. With XPS the coverage has been determined to be 0.25 on NiO (100). A detailed study has indicated that NO adsorbs on the terraces and not on the defect sides of the oxide surface [19].

On the polar NiO(111) surface it appears that adsorption of NO occurs on the Ni-terminated parts of the NiO(111) surface as opposed to the oxygen-terminated parts. The coverage is similar to NO on NiO (100). Even though a complete study of the adsorption behaviour for NO on NiO (111) has not yet been carried out, the TDS and XPS- results so far available are very similar to those found for NO adsorption on NiO(100).

3.2 Desorption dynamics NO/NiO(100)

Fig. 2 shows the determination of the desorption cross section both as measured on the surface via analysis of XP-spectra and in the gas phase via REMPI for the system NO/NiO(100) at T=100 K. In the left panel we determined the photodesorption cross section by XPS-measurements of the remaining coverage (N) after a certain photon exposure with respect to the initial coverage (N_o). The slope represents the photodesorption cross section. The value of $6*10^{-17}$ cm^2 is relatively large and within the experimental error identical with the one determined from the desorbed molecules in the gas phase (right panel) of $4*10^{-17}$ cm^2. The equivalence of cross sections determined on the surface and in the gas phase shows that the desorbing NO molecules are the majority species on the surface.

Fig. 3a) shows a set of velocity flux distributions for the desorbing NO molecules in one rotational state and three different vibrational states (v = 0,1,2). In Fig. 3b) we have plotted a set of velocity flux distributions for a fixed vibrational state and different rotational quanta from small to large values. Several issues are apparent:

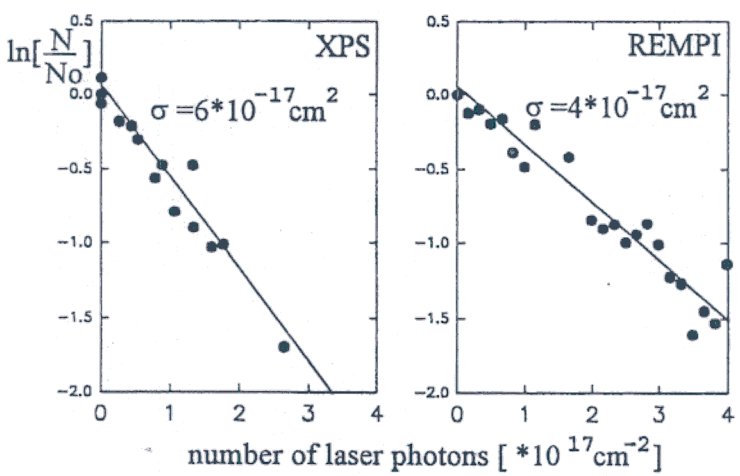

Fig. 2. Comparison of the desorption cross sections for the desorption of NO from NiO(100) measured via XPS (left side) and in the gas phase (right side).The logarithm of N/No is plotted against the number of photons.

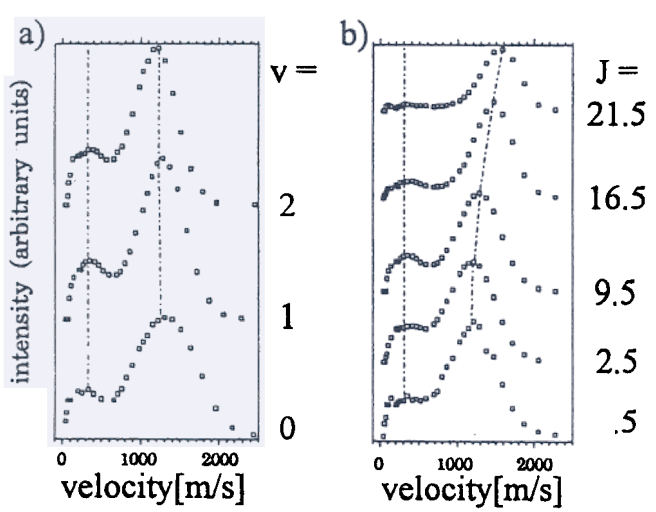

Fig. 3. Velocity flux distributions of desorbing NO from NiO(100).

a) Various vibrational states of one rotational state NO($^2\Pi_{3/2}$ J=11.5).

b) Various rotational quanta of the NO($^2\Pi_{3/2}$) for v =1.

i) The velocity distributions are bimodal (Fig.3).

ii) There is a coupling between rotational and translational motion for one of the maxima in the bimodal distributions (Fig.3.b).

iii) There is no obvious coupling of rotational and translational motion with vibration (Fig. 3.a). The molecules are vibrationally hot independent of whether they belong to the "slow" or the "fast" maximum of the bimodal distribution.

Neither the rotational nor the vibrational "temperatures" - if one wants to assign such a quantity - are directly connected with the surface temperature. The latter is about T = 120 K if we take the heating with the laser into account as estimated via the Bechtel-equation of heat flow [23]. The "slow" maximum in the velocity distribution exhibits the smallest "translational temperature" which is the region between 100 K < T < 200 K and thus close to the surface temperature. However, the "rotational temperature" is close to 400 K and the "vibrational temperature" around 1900 K. For the "fast" maximum the "translational temperature" varies between 1000 K < T < 2000 K as a function of the internal energy. For rotation and translation the values are comparable or even identical to those for the "slow" maximum. Clearly, it is not quite appropriate to use the term temperature in this connection the surface and the desorbing molecules are not equilibrated. The processes are of non-thermal origin.

3.3 Model Calculations

In order to explain the experimental observations we have carried out computer simulations of the desorption processes where we describe the excitation - deexcitation processes on the basis of quantum mechanical models and the propagation in the excited state as well as in the ground state potential quasiclassically [14,15]. We use the framework of the so called Menzel-Gomer-Readhead (MGR) model schematically shown in Fig. 4 [24,25].

Briefly, desorption is triggered by an electronic transition of the bound adsorbate-substrate complex. After the change of the potential energy curve has occurred the molecule propagates under the influence of the new potential energy curve for a time τ and may accumulate kinetic energy. After the time τ has elapsed the system relaxes into the ground state and transfers potential energy to the solid substrate via electron-hole-pair creation and/or phonon coupling. If the Franck-Condon concept is applied, the molecule keeps its kinetic energy, and if the accumulated kinetic energy is larger than the depth of the ground state well at the relaxation distance (Fig. 4), the molecule may escape the ground state well and desorption occurs.

To consider the dynamics of the molecule in the adsorbed state we use the model of the rigid rotor. This appears in the experimentally observed decoupling of the vibration and translation (see above). Fig. 5a illustrates typical motions of a molecule bound to the NiO(100) surface: In addition to the molecule-surface vibration a bending vibration of the molecule with respect to the surface may be excited. The vibration is fixed in amplitude to a region of solid angles by the angular dependence of the ground state potential (Fig. 5a). Due to these and possibly other motions a momentum k may be associated with the center of mass motion of the molecule in the ground state which is conserved during the electronic excitation of the molecule-surface complex [26]. With the assumption of an isotropic excited state potential, the electronic excitation leads to a rupture of the molecule-surface bond, i.e. the hindered rigid

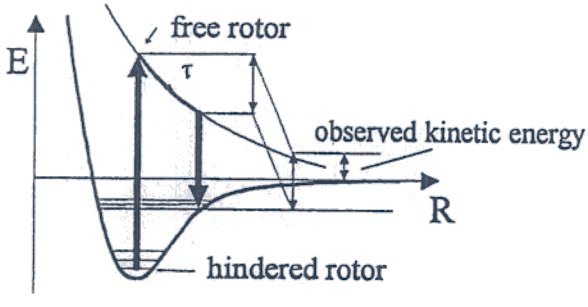

Fig. 4. MGR-model

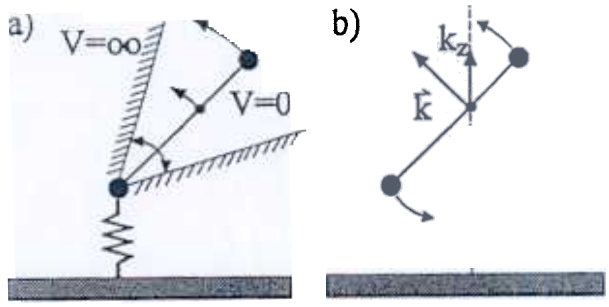

Fig. 5. Schematic representation of the models for the hindered rotor (a) and free rotor (b) as discussed in the text.

rotor in the adsorbed state becomes a free rigid rotor in the excited state [15]. The translational motion of the center of mass of the molecule may be characterized by the vector k (Fig. 5b). In case the electronic excitation occurs during the motion of the molecule away from the surface, k has a component pointing along the positive direction of the surface normal (k_z). In case it occurs while moving towards the surface, k has a component pointing along the negative direction of the surface normal.

The different signs of the k_z components have consequences for the desorption dynamics: For a repulsive excited potential, molecules with k_z components are moving away from the surface, while molecules with negative k_z are primarily moving towards the surface. After the initial momentum has been converted to potential energy, the molecules turn around and move outwards. Therefore, if the same lifetime in the excited state is chosen for all desorbing molecules, a molecule with an initially negative k_z component cannot acquire as much kinetic energy as a molecule with positive k_z. Consequently, relaxation to the ground state occurs at different positions on the potential energy surface. Thus the desorption dynamics will be different, which can lead for example to bimodal velocity (momentum) distributions. In other words, for a short lifetime of the excited state the relaxation occurs for both distributions at nearly the same position of the potentials and with nearly the same absolute values for k_z resulting in one peak of the momentum distribution after desorption. For longer lifetimes the relaxation of the two distributions occurs at different positions and with different absolute values of k_z, resulting in bimodal momentum distributions.

Generally, however, the observed behaviour strongly depends on the details (e.g. slope, existing minima, etc.) of the chosen excited state potential. We have sketched three typical situations in Fig. 6. The diagrams indicate that the molecules only probe a very limited region on the excited state potential where they are accelerated according to the slope of the potential. The observed velocity flux distribution is then strongly determined by the ground state potential. There are two issues to be adressed:

i) What is the nature of the repulsive potential energy curve?

ii) Why do we observe different populations in the two channels of the bimodal velocity flux distribution?

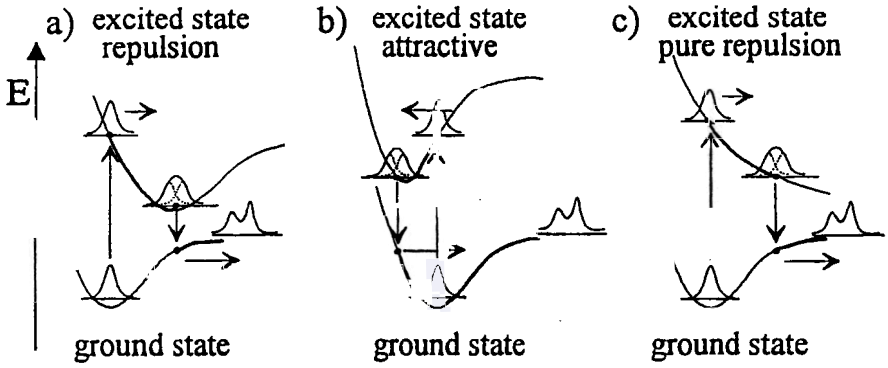

Fig. 6. Schematic drawing of three possible excitation processes with different excited states.

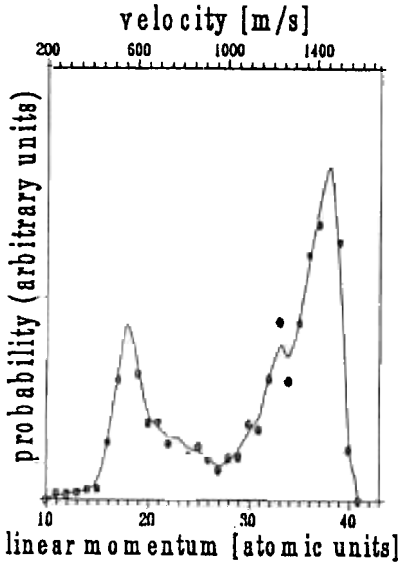

Fig. 7. Calculated velocity distribution

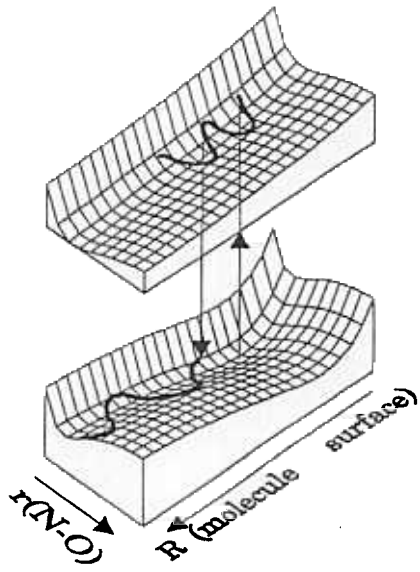

Fig. 8. Schematic representation of the potential energy surfaces.

i) Let us assume as the first elementary step the creation of an electron hole pair which initiates the electron to be charge transferred from the substrate to the molecule. In the literature there are some experimental indications that this is the situation encountered at the surface [12]. The excited state wavefunction of the adsorbed molecule would then look like a state of the NO^- ion. The remaining positive hole is screened on the oxide surface via the mobile electrons of the oxygen sublattice leading to an excited state potential with a minimum (Fig.6.a or b), the position of which depends on the details of the electronic interaction. However, upon excitation we assume that the molecules only probe the repulsive part of the excited state potential because of the short life time on the potential energy curve.

Therefore, we simulate this part of the potential curve by a repulsive 1/r-potential (Fig.6.c). We describe the rotational motion of the molecules on the excited state potential as a free rotor: if the interaction is basically electrostatic in nature it is reasonable to assume the potential to be isotropic. Therefore, in general the motion is thought to be more similar to a free than to a hindered rotor. Note, however, that the angular space probed by the molecule is small ($\Delta\Theta < 30°$) because the molecule has no time to fully rotate in the excited state. A model calculation where the parameters of the ground state potential [27] have been chosen according to existent experimental data leads to a typical time-of-flight distribution shown in Fig. 7. The lifetime enters as a parameter and was chosen as $\tau = 4 * 10^{-14}$ sec [15].

ii) The populations are governed by several factors, some of which are taken into account in the model calculations. Briefly, the probability to transfer from the excited state potential to the ground state will depend on the position on the excited state potential. Because the transfer occurs for the two components at different positions we expect differences in the populations. There is, however, another factor which has so far not been taken into account. The lifetimes of molecules initially moving inwards or outwards with respect to the surface may be different. This will lead to further changes in the relative populations. In fact, this latter aspect may turn out to be the more important one.

So far we have neglected the vibrations of the NO molecule in the adsorbate as well as in the desorbing particles. Our experimental results indicate that we can assume decoupling of rotation and translation from vibration. If we furthermore assume that the NO stretching vibration is decoupled from the NO-metal vibration we may find simple qualitative arguments to explain the observed vibrational excitations of the desorbing molecules. The situation is depicted in Fig. 8 where two potential energy surfaces (ground and excited states) are plotted as a function of the two independent degrees of freedom, namely the motion of the molecule away from the surface (R) and the NO stretching motion (r).

The excitation process may be described as follows: Before excitation the molecule is located in the global minimum of the lower curve. The photon excites the system via a Franck-Condon-like transition into the upper potential surface where the system only exhibits a minimum with respect to the NO stretching motion (r) and no minimum with respect to R. However, the position of the minimum as well as its shape differs from the situation in r-direction on the ground state potential energy surface. If we choose the potential well minimum to be located at larger distance, as would be the case if the nature of the excited state is NO^- like, the excitation leads to a non-eigenstate of the excited system in general. The propagation of this non-eigenstate may be described by solving the time dependent Schrödinger equation.

We assume to have significant quantum state populations at the surface just for v=0 in the ground state. Choosing the vibrational frequency from experimental data of various NO, or NO^+ and NO^- states [28] we may determine via a solution of the time-dependent Schrödinger equation a relaxation time τ after which for example the experimentally determined vibrational populations of the desorbing molecules are reproduced. A value that fits the populations is of the order of several 10^{-14} sec and thus compatible with the lifetime determined independently from the time-of-flight distribution [15]. Of course, the two life times do not have to correlate necessarily . However, in our case the hopping of the electron from the assumed NO^- back into the substrate triggers the formation of the observed neutral NO. Therefore the similarity of the two lifetimes is in favour of the proposed mechanism.

3.4 Desorption Dynamics NO/NiO(111)

As the next step we would like to investigate the applicability of our model for NO/NiO(111). However, the adsorbate NO/NiO(111) behaves differently compared with NO/NiO(100). In particular Fig. 9 b) shows that NO does not only desorb from the surface but also undergoes a chemical transformation on the surface. Before exposing to UV-radiation we find via XPS a N1s doublet typical for NO adsorbed on NiO(100). The fine structure is most probably due to a shake-up structure of a single species and not to the presence of two chemically different species [19].

In contrast to NO/NiO(100) the exposure of NO/NiO(111) to the UV-laserlight induces changes of the relative intensity of the two signals and not just a decrease of the intensity and we observe the build-up of a signal at 398.5 eV binding energy (Fig. 9a).

Apparently NO dissociates under UV-laser irradiation on NiO(111) leading to the formation of atomic nitrogen and oxygen (not detected) on the surface. The oxygen may react with excess NO to form NO_2 leading to a signal overlapping with the lower binding NO feature of the NO N1s-spectrum (402.3 eV). The atomic nitrogen remains at the surface. The assignment of the proposed NO_2 spectrum is corroborated by experiments where XP-spectra are taken

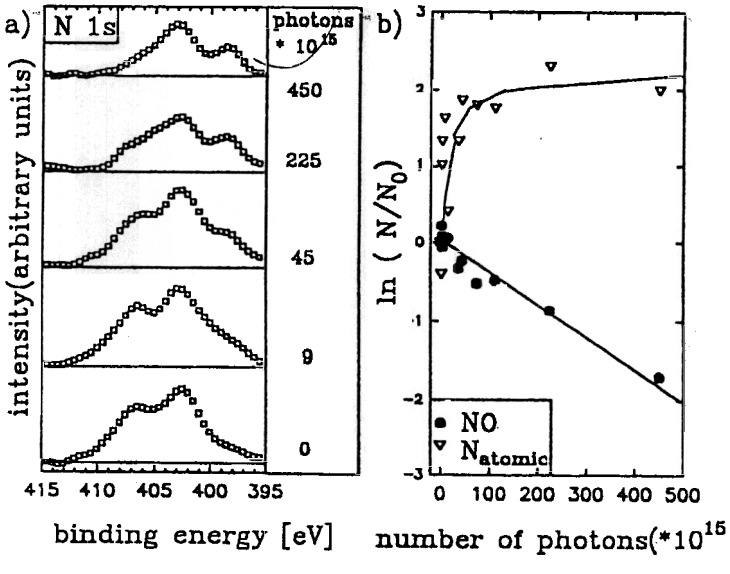

Fig. 9. Data for the laser induced desorption of NO from NiO(111).

a) A set of XPS-data for the N1s region after different numbers of photons exposed to the surface.

b) Logarithmic plot of $\ln(N/N_0)$ versus the number of photons. The filled circles refer to the signal at 406.7 eV (pure NO) and the open triangles belongs to the signal of atomic nitrogen at 398.5 eV.

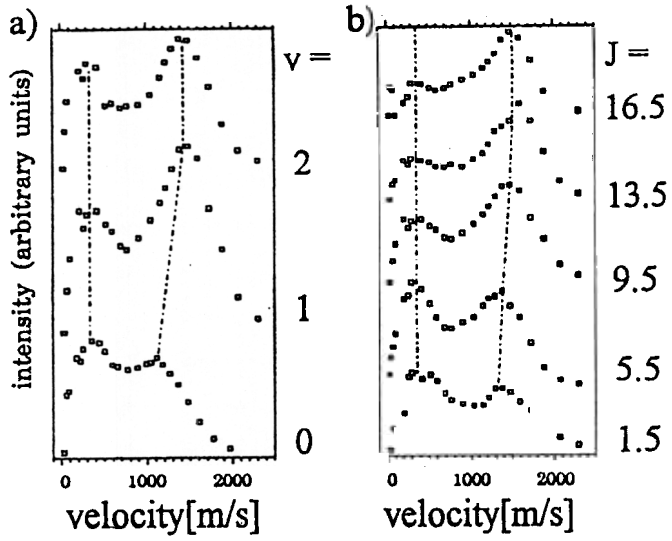

Fig. 10. Velocity distributions of desorbing NO from NiO(111).
a) Various vibrational states of one rotational state NO($^2\Pi_{3/2}$ J=11.5).
b) Various rotational quanta of the NO($^2\Pi_{3/2}$) for v =1.

after direct NO_2 adsorption on NiO(100) leading to a signal at 403.1 eV binding energy [29]. Therefore in our further discussion we will assign the reaction product as being NO_2. Further spectroscopic measurements in order to finally identify the reaction product have to be undertaken. Summarizing so far in contrast to NO/NiO(100), where only desorption can be observed, for NO/NiO(111) we also find a reaction channel for NO dissociation.

In Fig.9 b) ln (N/N_0) for the system NO/NiO(111) is plotted versus the number of photons exposed to the surface as obtained from an analysis of the XP-spectra. The plot reveals that the coverage of the atomic nitrogen saturates at the surface. However, the cross section observed in the gas phase is a result of the combined processes, namely the photoreaction and the photodesorption. We have investigated the velocity distributions for different vibrational and rotational quanta of the NO desorbing from NiO(111). These are shown in Fig. 10. Again we observe bimodal velocity distributions with velocity values similar to the NO desorbing from NiO(100), but the relative population of the "fast" and "slow" features are different for a given rotational state and varying vibrational state. The velocities only vary moderately. The rotational and vibrational temperatures are rather similar. The velocities of the "fast" channel for v=1 and v=2 are equal (about 1300 m/s), but the velocity in v=0 is smaller (1050 m/s). In addition we find strong coupling between translational and rotational motion in v=0 (900 - 1400 m/s), however the coupling is weak in the excited vibrational states (1300-1500 m/s).

The higher vibrationally and rotationally excited the desorbing NO-molecules are, the more similar the velocity flux distributions become to those for NO desorbing from NiO(100). The distributions show comparable positions of their maxima and of their populations. The velocity distributions are a result of two different channels (photodesorptive and photochemical). Further investigations are in progress in order to find out about the contributions of the two channels to the final velocity distributions.

We have also investigated the laser induced desorption of CO. On NiO(111) CO is adsorbed below 160 K in contrast to NiO(100) where it does not adsorb as revealed by XPS and TDS. Similar to the case of NO on NiO(100) CO desorbs without reaction with a cross section of the same order of magnitude.

Acknowledgements

We thank the Deutsche Forschungsgemeinschaft as well as the Ministerium für Wissenschaft und Forschung for financial support. H.-J. F. thanks the Fonds der Chemischen Industrie.

Literature:

1. X.L. Zhou, X.-Y. Zhu, J.M. White, Surf.Sci.Rep. **13** ,77(1991).
2. W. Ho, Desorption Induced by Electronic Transitions, DIET IV, Springer Ser.Surf.Sci. **19**, 48, Berlin, Springer-Verlag (1990).
3. A. Mödl, T. Gritsch, F. Budde, T.J. Chuang, G.Ertl, Phys.Rev.Lett. **57**, 384 (1986).
4. A.R. Burns, E.B. Stechel, E.R. Jennison, Phys.Rev.Lett. **58**, 250 (1987); E.B. Stechel, D.R. Jennison, A.R. Burns, Desorption Induced by Electronic Transitions, DIET III, Springer Ser.Surf.Sci.**13**, 137, Berlin, Springer-Verlag (1988); D.R. Jennison, E.B. Stechel, A.R. Burns, ibid., p.167
5. D. Weide, P. Andresen, H.-J. Freund, Chem.Phys.Lett. **136**, 106 (1987).
6. F. Budde, A.V. Hamza, P.M. Ferm, G. Ertl, D. Weide, P. Andresen, H.-J. Freund, Phys.Rev.Lett. **60**, 1518 (1988).
7. W.C. Natzle, D. Padowitz, S.J. Sibener, J.Chem.Phys. **88**, 7975 (1988).
8. E. Hasselbrink, S. Jakubith, S. Nettesheim, M. Wolf, A. Cassuto, G. Ertl, J.Chem.Phys. **92**, 3154 (1990).
9. M. Wolf, E. Hasselbrink, J.M. White, G. Ertl, J.Chem.Phys. **93**, 5327 (1990).
10. R. Schwarzwald, A. Mödl, T.J. Chuang, Surf.Sci. **242**, 437 (1991).
11. K. Mase, S. Mizuno, Y. Achiba, Y. Murata, Surf.Sci. **242**, 444 (1991).
12. J.W. Gadzuk, L.J. Richter, S.A. Buntin, D.S. King, R.R. Cavanagh, Surf.Sci. **235**, 317 (1990).
13. Th. Mull, H. Kuhlenbeck, G. Odörfer, R. Jaeger, C. Xu, B. Baumeister, M. Menges, G. Illing, H.-J. Freund, D. Weide, P. Andresen, Desorption Induced by Electronic Transitions, DIET IV, Springer Ser.Surf.Sci. **19**, 169, Berlin, Springer-Verlag (1990).
14. B. Baumeister, M. Menges, T. Mull, H.-J. Freund, D. Weide, P. Andresen, Proceedings of the Symposium on Surface Science, La Plagne, France, p. 147 (1990).
15. Th. Mull, B. Baumeister, M. Menges, H.-J. Freund, D. Weide, C. Fischer, P. Andresen, J.Chem.Phys., **96**, 7108 (1992).
16. J. Yoshinobu, T.H. Ballinger, Z. Xu, H.J. Jänsch, M. I. Zaki, J. Xu, J.T. Yates Jr., Surf.Sci **255**,295 (1991).
17. M. Asscher, F.M. Zimmermann, L.L. Springsteen, P.L. Houston, W. Ho, submitted.
18. Th. Mull, Ph. D. Thesis, Bochum (1991).
19. H. Kuhlenbeck, G. Odörfer, R. Jaeger, G. Illing, M. Menges, Th. Mull, H.-J. Freund, M. Pöhlchen, V. Staemmler, S. Witzel, C. Scharfschwerdt, K. Wennemann, T. Liedtke, M. Neumann, Phys.Rev. **B 43**, 1969 (1991).
20. E. Escalona Platero, C. Coluccia, A. Zecchina, Langmuir **1**, 407 (1985).
21. M. Bäumer, D. Cappus, H. Kuhlenbeck, H.-J. Freund, G. Wilhelmi, A. Brodde, H. Neddermeyer, Surf.Sci. **253**, 116 (1991).
22. M. Bäumer , D. Cappus, G. Illing, H. Kuhlenbeck, H.-J. Freund, J.Vac.Sci.Technol. **A 10**, 1 (1992).
23. J.H. Bechtel, J.Appl.Phys. **46**, 1585 (1975).
24. D. Menzel, R. Gomer, J.Chem.Phys. **41**, 3311 (1964).
25. P.A. Redhead, Can.J.Phys. **42**, 886 (1964).
26. U. Landman, Israel J.Chem. **22**, 339 (1982).
27. J.E. Smedley, G.C. Corey, M.H. Alexander, J.Chem.Phys. **87**, 3218 (1987).
28. K.P. Huber, G. Herzberg, "Molecular spectra and molecular structure. Vol. 4: Constants of diatomic molecules", Van Nostrand Reinhold Company, New York 1979.
29. M. Menges, Diplomarbeit, Bochum 1990.